# An Update to Patricio de la Cuadra's Lumped Element Model of the Flute

Regina Collecchia

June 11, 2013

## 1 Abstract

This project is based mostly on Patricio de la Cuadra's 2005 thesis research on physically modeling flutes. His model incorporates the aeroacoustic sources of jet drive, turbulence, and voriticty as lumped elements into the excitation, which forms a feedback loop with the resonator of the flute. Cuadra's research culminated in several software implementations of his model, namely in the open source software Pure Data which was then converted into a Max/MSP object (i.e., class) and synthesizer. Since Max/MSP has recently undergone changes that make rigorous, efficient signal processing on audio samples themselves, an updated version of Cuadra's patch was undertaken, using the new MSP object gen . Though not completed, the CPU usage of the updated patch has been reduced 4-fold henceforth, with most of it going to a spectrometer.

## 2 Introduction

Physically modeling musical instruments started with finite difference approximations of the wave equation, but really accelerated at the Center for Computer Research in Music and Acoustics in the 1980s. Julius O. Smith III developed very fast algorithms for very slow computers: the Karplus-Strong algorithm and digital waveguide synthesis. These algorithms enable real-time synthesis methods—a necessity to any musician wishing to perform live with them (as opposed to theoretical analysis)—and when combined with their believable output and mathematical elegance, have been hard to beat.

However, digital waveguides are only one-dimensional, and therefore are only an approximation to musical instruments which radiate three-dimensionally. For wind instruments this is especially true, as the width and length of a violin's string is closer to an ideal waveguide than the geometry of a saxophone's bore. Besides that, computers are actually fast now and able to tackle much bigger problems.

Integral models of vortex shedding (e.g., Howe [5]) come closer to accurately modeling the physical behavior of flutes, though they do assume an incompressible flow. Probably due to the fact that aeroacousticians are more interested in solving jet engine noise than problems that have pretty much been solved, not many implementations of aeroacoustic approaches to musical problems exist to date. Furthermore, integral models are typically only valid for idealized geometries (such as infinite thinness or punctual vortices) and an enormous jump in complexity from a wave that only propagates to the left and right with one multiply in between them.

Cuadra found a compromise. He augments a lumped element model of the flute with aeroacoustic sources in the excitation.

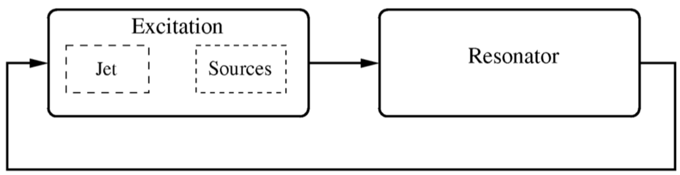


**Figure 1:** The simplest depiction of Cuadra's model. The jet, filter of the mouth, and the aeroacoustic sources sum together as lumped elements, and excite the resonator. Image from [1].

Cuadra's dissertation culminated in a C++ class in Smith and Cook's Synthesis Tool Kit as well as Pure Data and Max/MSP objects with many parameters, especially focusing on the aeroacoustic variables. Cuadra made the Max/MSP available to me (but not the source code of his Max object) and it is indeed a very dynamic flute synthesizer. His specific flute of interest was the European transverse flute. He performed experimental measurements on this instrument which included video recordings of his lips while performing, a pressure sensor inside his mouth, and image processing of videos to ascertain the mass density gradient $\partial\rho$ of the air, visualized using the Schlieren method (Fig. 2).

This determined the lip hole geometry $h \times H$ (and surface area $S_m$), pressure inside the mouth $p_m$, and the **jet central velocity** $U_j$. As we shall see, these three variables alone solve almost every governing equation in this model.

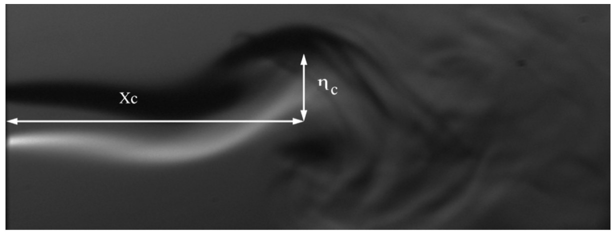


**Figure 2:** Oscillations of the jet are visualized using the Schlieren technique.

# 3 Lumped element model with aeroacoustic sources

The input pressure is typically computed by assimilating physical objects such as masses, dashpots, and springs to resistors, capacitors, and inductors, and then solving the transfer function. But since we have a measured input pressure, this is not

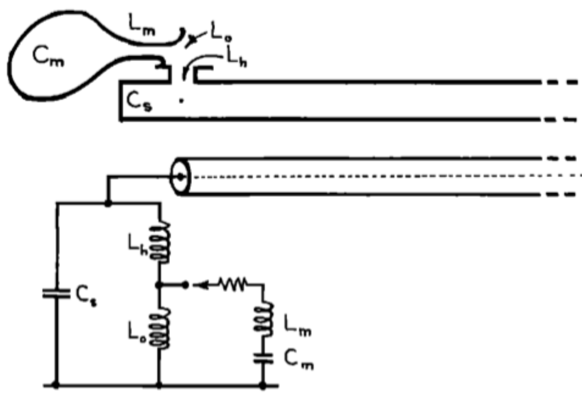


**Figure 3:** The flute embouchure-hole system (from [2]) and its equivalent electrical circuit.

necessary.

## 3.1 The excitation

The excitation initiates from the mouth of the performer into the **chimney** of the flute. We call their coupling the **formation channel**, where the jet is initiated. The jet reaches the **labium** of the flute, a sharp edge (similar to a reed) which produces the Bernoulli effect, and this excites standing waves in the resonator.

After measuring $p_m$, Cuadra went on to separate it into its slowly and quickly moving components, $P_m$ and $p'_m$, where $p_m$ and $p'_m$ oscillate at the (measurable) fundamental frequency $f_0$. The slow component $P_m = p_m - p'_m$ is simply the pressure

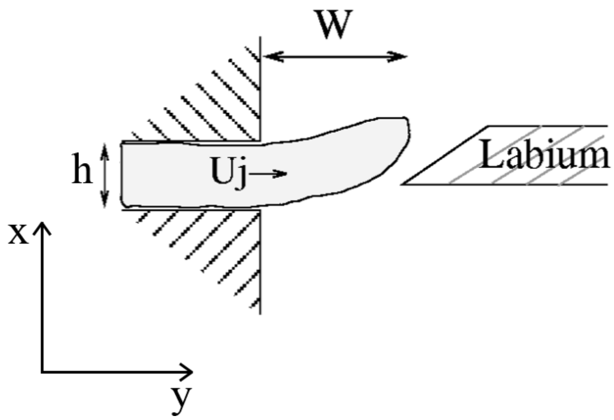


**Figure 4:** Excitation parameters, modified from [1]. $W$ is the **flue-labium distance** (which is also the distance from the end of the **formation channel**) and $h$ is the **jet height**.

difference along the jet path at the mouth hole. Any space between the performer's lips and the mouthpiece will damp the energy of $f_0$.

### The jet

The **jet velocity profile** is assumed to be Bickley:

$$U(Y) = U_j \operatorname{sech}^2\left(\frac{y}{b}\right) \tag{1}$$

where $b = \frac{2h}{5}$, $h$ the **jet height**.

Since the path of the jet at the mouth is very short, we may assume that the flow boundaries are negligible. Therefore, we can check the measured $U_j$ with the theoretical jet velocity determined by the Bernoulli equation, wherein

$$U_j = \sqrt{\frac{2P_m}{\rho_0}}. \tag{2}$$

$U_j$ will be different towards the edges of the bore due to viscosity, so this only applies to the velocity at the center of the jet.

Sound generation in the flute also comes from a **transverse acoustic velocity** in the $x$ direction, $V_{ac}$. The **transverse displacement** of the jet is also dependent on the frequency of oscillation:

$$\eta(x,\omega) = \frac{V_{ac}}{i\omega}\left[1-\cosh(\alpha x)e^{-i\omega(t-x/c_p)}\right] \tag{3}$$

$$\approx \eta_0 e^{\alpha_i x}\ e^{i\omega(t-x/c_p)} \tag{4}$$

with propagation velocity $c_p$. We use this approximation because the jet is perturbed at the labium, and the amplitude of the perturbation grows exponentially ($\alpha > 0$) as it travels from the channel exit, as shown in Fig. 2. It should also be noted that all sound produced by non-stationary flow is localized at the labium.

We know that the velocity of the excitation is sinusoidal because it is compressible. Euler's relation says that

$$-\rho_0\frac{dv}{dt} = \frac{\partial P}{\partial y}. \tag{5}$$

Therefore, $v = V_{ac}e^{-j\omega t}$, and the amplitude of the acoustic velocity in the excitation is

$$V_{ac} = \frac{1}{i\omega\rho}\frac{\partial p}{\partial y} \tag{6}$$

$$= \frac{p_0-p_1}{\rho_0 c}, \tag{7}$$

the difference of the input and output pressure divided by the mass density of air $\rho_0 = 1.2$ kg/m$^3$ and speed of sound in air $c = 343$ m/s. For normal playing conditions,

$$\left|\frac{V_{ac}}{U_j}\right| \approx 0.1. \tag{8}$$

### Aeroacoustic sources

There are 3 aeroacoustic sources considered by Cuadra that feed into the resonator after summing together with the jet impulse: **jet drive**, **vortices**, and **turbulences**. They are related to the **receptivity** and the **instability** of the jet. Receptivity is the jet's reaction to the acoustic excitation, quantified above by the transverse displacement $\eta$. Instability is a function of receptivity, defining the**perturbations** on the jet as a function of $x$. The propagation velocity of these perturbations is about $U_j/2$.

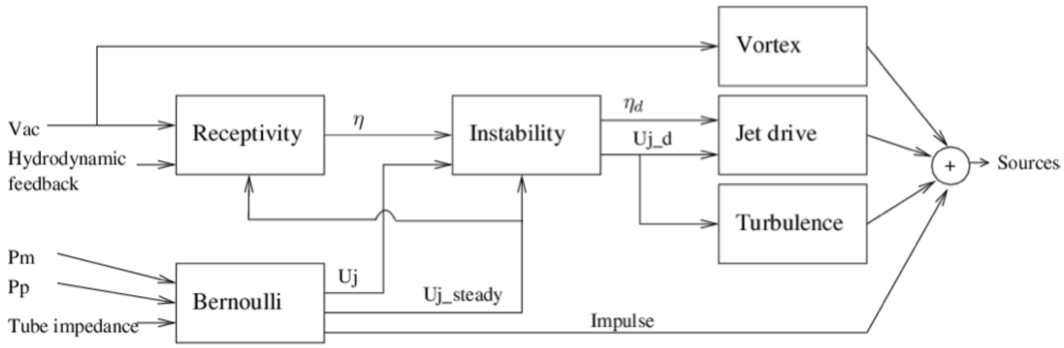


**Figure 5:** Block diagram of the sources, which is then input into the resonator.

1. **Jet drive**. The jet drive is the transfer of energy from the jet to the resonator. The total flow feeding into the resonator is

$$\begin{aligned} Q_{in} &= \int_{-\infty}^{\eta - y_0} U_j(y)\, dy && (9) \\ &= bHU_0 \left[ 1 + \tanh\left( \frac{\eta - y_0}{\psi b} \right) \right] && (10) \end{aligned}$$

where $y_0$ is the position of the jet with respect to the vertical center of the formation channel, $H$ is the width of the lips' hole, and $\psi$ is a parameter that allows the jet shape (width) to be controlled.

2. **Vortices**. These are present in (a) the shear layers of the jet, (b) the place of jet interaction with the labium, and (c) the flow that escapes the mouth of the instrument because of space between the performer's lips and the mouthpiece. Parts (a) and (b) inject energy into the resonator, while (c) damps the energy of the fundamental. The vortices are responsible for energy in the high harmonics, and non-linearities in the flute.

   (a) The average power generated by the shear layers over one period of oscillations $T$ is

$$P_{av} = -\frac{\rho}{T} \int_0^T \int_V (\omega \times V_{ac}) v_y \, dV \, dt \qquad (11)$$

   for the source volume $V$ and velocity $u'$, the unsteady part (not oscillating at $f_0$) of $V_{ac}$.

(b) Probably because it is very difficult to make measurements inside of the flute, Cuadra does not give a function for this source, and neglects it in his model.

(c) We model a pressure jump across the mouth of the instrument:

$$\Delta p_m = -\frac{\rho}{2}\left(\frac{V_{ac}}{\alpha_v}\right)^2 \mathrm{sign}(Q_p) \tag{12}$$

where $\alpha_v$ is a scalar between 0.6 and 1.

3. **Turbulences**. Most classical music for flute is ideally played with no or very low turbulence, to get a crisp, clear tone. They occur after the vortex street (the perturbations) created by the jet. Bechert [6]

## 3.2 The resonator

The flute's resonator is modeled as a 3-port scattering junction, describing the reflection and transmission interactions between the chimney, upper cavity, and bore. The losses filter $l(t)$ is given by the difference equation

$$l(t) = (1 - b_L)\, g_l x(t) + b_L\, l(t-1) \tag{13}$$

where $b_L = 0.6$, the coefficient of the frequency-dependent loss filter, and $g_l = 0.94$, the gain of the loss. The end reflection filter $r(t)$ is computed in the left ($x$) and right ($y$) directions:

$$r(t)_y = b_{R0}\, l(t) + b_{R1}[r(t)_x - r(t)_y], \tag{14}$$
$$r(t)_y = l(t) \tag{15}$$

where $b_{R0} = -0.4793$ and $b_{R1} = -0.2603$.

The **impedance** at the end of the bore is akin to a circular piston with radius $a$:

$$\mathbf{Z}_r = \frac{\rho_0 c}{S}[R_r(2ka) + iX_r(2ka)] \tag{16}$$

where $S = \pi a^2$ and

$$R_r(x) = 1 - \frac{2J_1(x)}{x} \tag{17}$$
$$X_r(x) = \frac{2H_1(x)}{x} \tag{18}$$

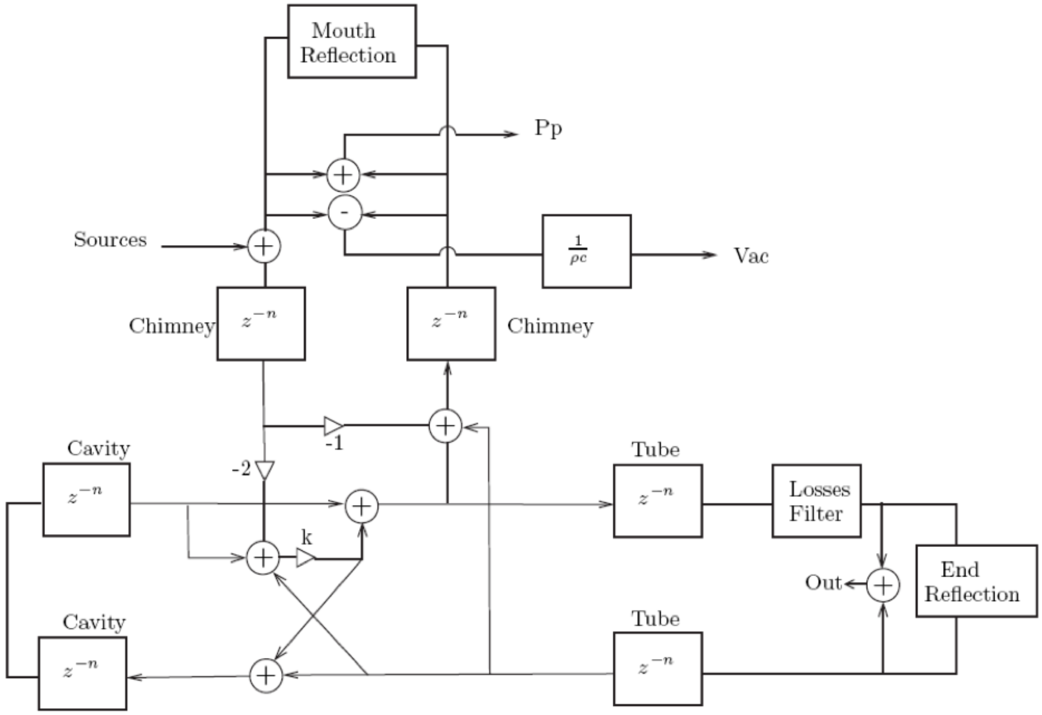


**Figure 6:** The 3-port scattering junction of the flute resonator (body), given in [1]. $P_p$ is the mouth pressure. $V_{ac}$ is the acoustic velocity. "Sources" shows the excitation point, and "Out" is at the end of the bore where most of the sound is radiated.

$J_1$, $H_1$ the first-order Bessel and Struve functions. For low frequencies ($ka << 1$), they no longer depend on $x$:

$$R_r \approx \frac{1}{2}\rho_0 c S(ka)^2 \tag{19}$$

$$X_r \approx \frac{8}{3\pi}\rho_0 c S(ka) \tag{20}$$

Then, the reflection coefficient at the end of the bore is

$$\Gamma = \frac{\mathbf{Z}_r - 1}{\mathbf{Z}_r + 1}. \tag{21}$$

# 4 Software implementation

The resonator was successfully modeled using gen$\sim$ in Max 6, and does by itself produce an already flute-like timbre. I was able also to approximate the aural effect of turbulence just by making the excitation a linear combination of noise and sinusoidal pressure.

My model may or may not turn out to be more efficient than the model he produced in 2005 in Pure Data, since he wrote an object **flauta_pd∼.mxo** in C++, but at the present it only uses about 1.7% of my CPU, on a 2008 MacBook Pro with a 2.4 GHz Intel Core 2 Duo processor. Cuadra's Max patch uses about 7%.

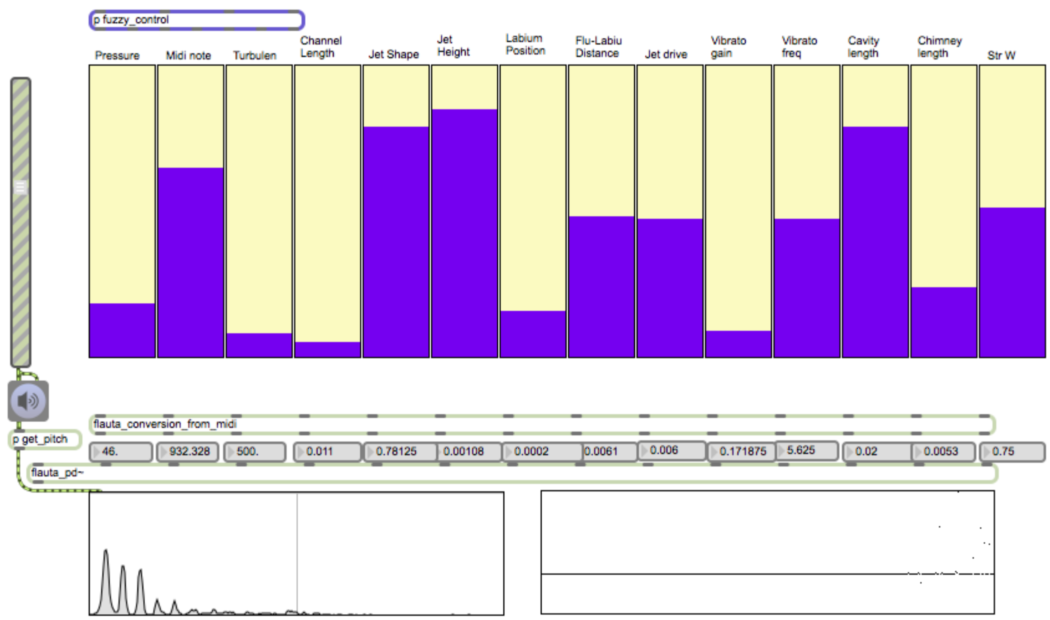


**Figure 7:** The Max 4 patch (ported from Pure Data) implementation by Cuadra. The object **flauta_pd∼** is coded in C++.

Within this patch is a "subpatcher" **p fuzzy_control**, and inside that, the subpatch **fuzzy_patch**, containing another Max object created by Cuadra called **fuzzy**:

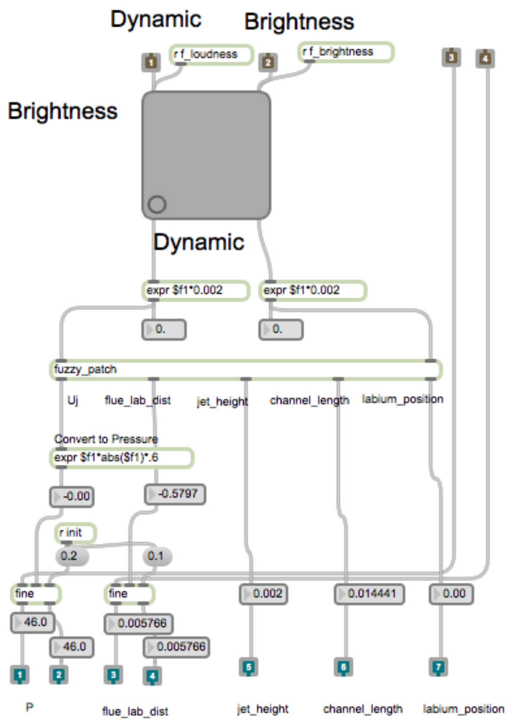


**Figure 8:** The subpatch **p fuzzy_control**, which converts the jet central velocity $U_j$ to pressure by the equation $b_L U_j \overline{U_j}$.

## 4.1 Parameters of Cuadra's patch

- **Input pressure from the mouth** $p_m$. The input pressure affects which harmonics are most pronounced. As $p_m$ increases, the fundamental may shift up a harmonic, or even 3 harmoniics (to $4f_0$). The energy of the harmonics also increases proportionally to $p_m$.
- **Fundamental frequency** $f$. For the flute, this is in the range $30 \leq f \leq 11000$.
- **Turbulence**. This is the **Reynolds number** $Re$, which describes the "type" of jet. It is minimal for the recorder and maximal for the transverse flute:

$$500 < Re = \frac{U_j h}{\nu} < 10,000 \tag{22}$$

where $\nu = 1.5 \times 10^{-5}\ m^2/s$ is the kinematic viscosity of the air. The transition

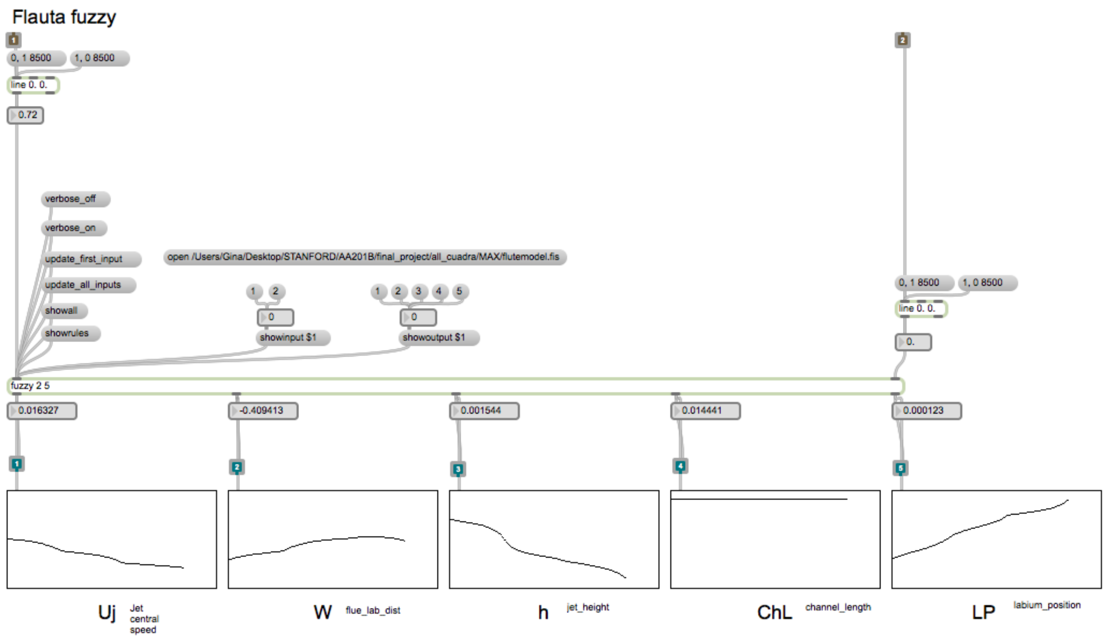


**Figure 9:** The object **fuzzy** with arguments 2 (the number of inlets) and 5 (the number of outlets. It computes $U_j$, $W$, $h$, the channel length, and the labium position as functions of the frequency loudness and "brightness".

from a laminar to turbulent jet occurs somewhere in the range $2500 < Re < 3000$.

- **Formation channel length**. Not all flutes have the same channel length. This number ranges between 1 and 10 mm. The shorter the length, the higher the gain.
- **Jet shape** $\psi$. This falls in the range $0 \leq \psi \leq 1$.
- **Jet height** $h$ and **flue-labium distance** $W$. The ratio of the jet geometry typically falls in the range

$$3 < \frac{W}{h} = \frac{Str_W}{Str_h} < 12 \tag{23}$$

where the lower end represents thicker jets as seen in the transverse flute. The jet height is typically 1 mm. The maximum jet instability occurs at $Str_h \approx 0.03$ indicating that $W/h = 8$. Organ pipes can have a ratio as high as 16.

- **Labium position**. This determines where the resonator is excited. It is located underneath the mouthpiece, offset no more than 1.27 mm from there for the flutes Cuadra considered.

- **Jet drive**. Also, $U_j \approx 3$ m/s when the jet is laminar, and greater when it is turbulent.

- **Vibrato gain and frequency** $g_v$, $f_v$. Vibrato adds a pleasant texture to the flute sound and is frequently employed by flautists.

- **Cavity and chimney length**. The length of the bore is 60 cm; I am

- **Strouhal number** $Str$. This describes the flow instability along its height and width.

$$Str_W = \frac{fW}{U_j} \tag{24}$$

$$Str_h = \frac{fh}{U_j}. \tag{25}$$

  In normal playing conditions, the distance $W$ between the flue exit and the labium is about half the hydrodynamic wavelength $\lambda_h$. Therefore, $Str_W \approx 0.25$.

# 5 Conclusions and future work

Cuadra's success has given me faith that aeroacoustic sources contribute significantly to the timbral range of the flute. I originally planned to do something with an integral model, but the accessibility of the equations in his dissertation was very appealing to my level of knowledge in aeroacoustics.

With regards to the software, I later today realized that the "fuzzy" object in Cuadra's Max patch had a hard-coded file path, so the demonstration I gave of it during my presentation was probably not varying the aeroacoustic sources. I still have plenty to do in my own patch, as indicated in the "TODO" list in Fig. 10.

I am also working on a patch with visiting professor Robert Henke that actually exploits some of the sounds that aren't so flute-like, that emerge occasionally from all of these models.

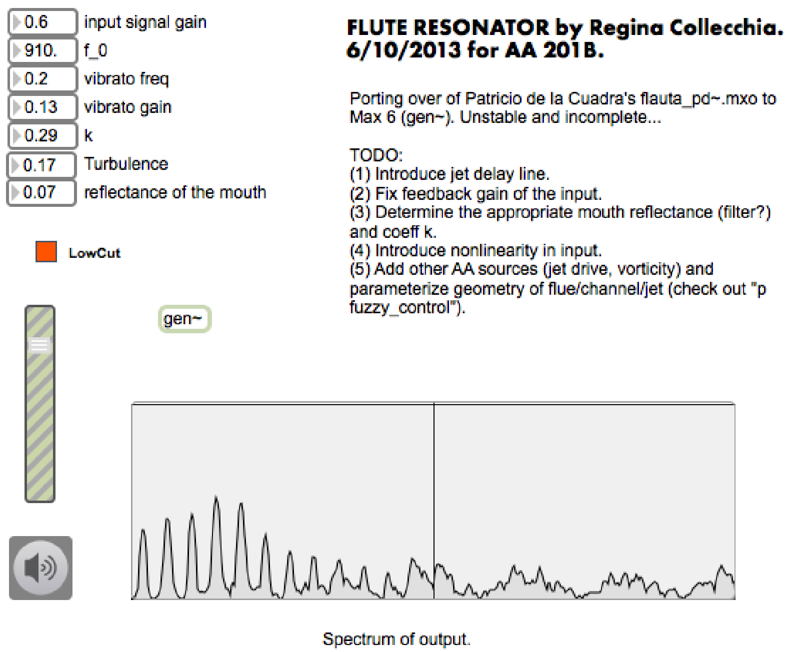


**Figure 10:** My (incomplete) Max patch that redoes Cuadra's work from scratch.

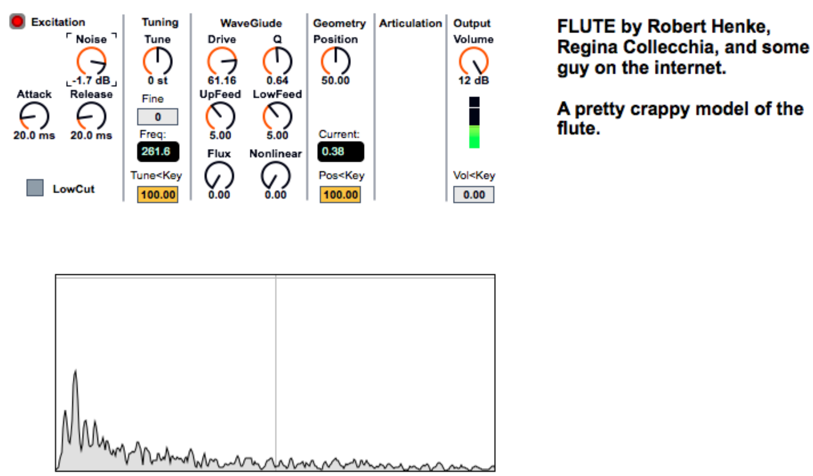


**Figure 11:** Collaboration between Robert Henke and I on another LEM flute patch that started from some code he found online. It includes a resonant bandpass filter that is problematic, as $Q$ shifts $f_0$, as well as phase modulation that shifts phase according to the delay time, which we believe to be flawed.

# References

[1] P. de la Cuadra. "The Sound of Oscillating Air Jets: Physics, Modeling and Simulation in Flute-Like Instruments." Doctoral dissertation, Stanford University. 2005.

[2] A.H. Benade, J.W. French. "Analysis of the flute head joint." In *J. Acoust. Soc. Am.*, **37**(4):679–691. 1965.

[3] M. van Walstijn, G. Scavone. "The wave digital tonehole model." In *Proc. of International Comp. Music Conf. ICMC-2000*, 465–468. 2000.

[4] B. Fabre, J. Gilbert, A. Hirschberg, and X. Pelorson. "Aeroacoustics of Musical Instruments." In *Annual Review of Fluid Mechanics*, 44:1–25. 2012.

[5] M.S. Howe. "Contribution to the theory of aerodynamic sound, with application to excess jet noise and the theory of the flute." In *J. Fluid Mech.*, 71:625–673. 1975.

[6] D.W. Bechert. "Excitation of instability waves in free shear layers part 1: theory." *J. Fluid Mech.*, 186:47–62. 1988.

[7] J.W. Coltman. "Sounding mechanism of the flute and organ pipe." In *J. Acoust. Soc. Am.*, 44:983–992. 1968.

[8] J.W. Coltman. "Resonance and sounding frequencies of the flute." In *J. Acoust. Soc. Am.*, 40:99107. 1966.

[9] M.P. Verge. *Aeroacoustics of Confined Jets, with Applications to the Physical Modeling of Recorder-Like Instruments.* Doctoral dissertation, Technische Universiteit Eindhoven. 1995.

[10] P. Dickens. "Flute acoustics: measurement, modelling and design." Doctoral dissertation, University of New South Wales. 2007.